Hindawi Publishing Corporation
EURASIP Journal on Wireless Communications and Networking
Volume 2007, Article ID 37574, 9 pages
doi:10.1155/2007/37574

Research Article

Diversity Characterization of Optimized Two-Antenna Systems for UMTS Handsets

A. Diallo,[1] P. Le Thuc,[1] C. Luxey,[1] R. Staraj,[1] G. Kossiavas,[1] M. Franzén,[2] and P.-S. Kildal[3]

[1] *Laboratoire d'Electronique, Antennes et Télécommunications (LEAT), Université de Nice Sophia-Antipolis, CNRS UMR 6071, 250 rue Albert Einstein, Bât. 4, Les Lucioles 1, 06560 Valbonne, France*
[2] *Bluetest AB, Gotaverksgatan 1, 41755 Gothenburg, Sweden*
[3] *Department of Signals and Systems, Chalmers University of Technology, 41296 Gothenburg, Sweden*

Received 16 November 2006; Revised 20 June 2007; Accepted 22 November 2007

Recommended by A. Alexiou

This paper presents the evaluation of the diversity performance of several two-antenna systems for UMTS terminals. All the measurements are done in a reverberation chamber and in a Wheeler cap setup. First, a two-antenna system having poor isolation between its radiators is measured. Then, the performance of this structure is compared with two optimized structures having high isolation and high total efficiency, thanks to the implementation of a neutralization technique between the radiating elements. The key diversity parameters of all these systems are discussed, that is, the total efficiency of the antenna, the envelope correlation coefficient, the diversity gains, the mean effective gain (MEG), and the MEG ratio. The comparison of all these results is especially showing the benefit brought back by the neutralization technique.

1. INTRODUCTION

Nowadays, wireless mobile communications are growing exponentially in several fields of telecommunications. The new generation of mobile phones must be able to transfer large amounts of data and consequently increasing the transfer rate of these data is clearly needed. One solution is to implement a diversity scheme at the terminal side of the communication link. This can be done by multiplying the number of the radiating elements of the handset. In addition, these radiators must be highly isolated to achieve the best diversity performance. Also, the antenna engineers must take into account the radiator's environment of the handset to design suitable multiantenna systems. In practice, the terminal can be considered to operate in a so-called multipath propagation environment: the electromagnetic field will take many simultaneous paths between the transmitter and the receiver. In such a configuration, total efficiency, diversity gain, mean effective gain (MEG), and MEG ratio are the most important parameters for diversity purposes.

Only few papers are actually focusing on the design of a specific technique to address the isolation problem of several planar inverted-F antennas (PIFAs) placed on the same finite-sized ground plane and operating in the same frequency bands. In [1, 2], the authors are evaluating the isolation between identical PIFAs when moving them all along a mobile phone PCB for multiple-input multiple-output (MIMO) applications. The same kind of work is done in [3–6] for different antenna types. The best isolation values are always found when the antennas are spaced by the largest available distance on the PCB, that is, one at the top edge and the other at the bottom. Excellent studies can be found in [7–16], but no specific technique to isolate the elements is described in these papers. One solution is reported in [17], however, for two thin PIFAs for mobile phones operating in different frequency bands (GSM900 and DCS1800). It consists in inserting high-Q-value lumped LC components at the feeding point of one antenna to achieve a blocking filter at the resonant frequency of the other. This solution gives significant results in terms of decoupling but strongly reduces the frequency bandwidth. Another very interesting solution reported in [18, 19] consists in isolating the antennas by a decoupling network, at their feeding ports, this solution suffers from the fact that in small handsets available space is restricted. Finally, a promising solution is described in [20], but in this work the PIFAs are operating around 5 GHz.

Some authors of the current paper have already designed and fabricated several multiantenna structures for mobile

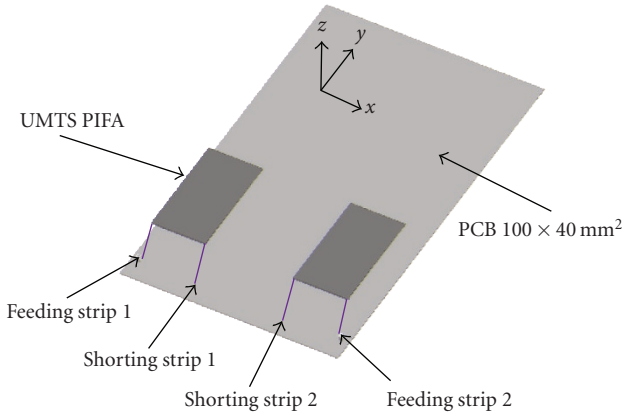

Figure 1: 3D view of the initial two-antenna system.

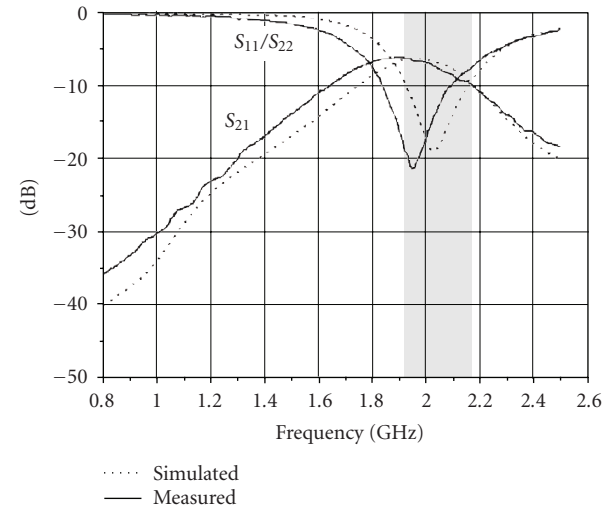

Figure 2: Simulated and measured S-parameters of the initial two-antenna system.

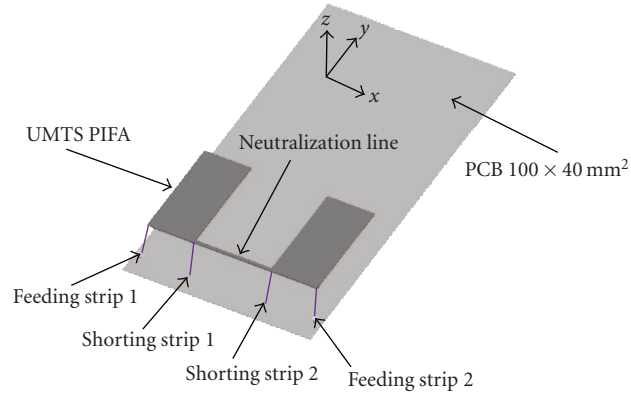

Figure 3: 3D view of the two-antenna system with a suspended line between the PIFA shorting strips.

phone applications. In [21], the isolation problem has been addressed for closely spaced PIFAs operating in very close frequency bands with the help of a neutralization technique. Recently, several two-antenna systems operating in the UMTS band (1920–2170 MHz) and especially including neutralization line to achieve high isolation between the feeding ports of their radiating parts have been designed for diversity and MIMO applications [22]. Two prototypes have already been characterized in terms of scattering parameters, total efficiency, and envelope correlation coefficient. The obtained results show that these structures have a strong potential for an efficient implementation of a diversity scheme at the mobile terminal side of a wireless link. However, to completely characterize these prototypes, some particular facilities and the associated expertise are needed [23]. The antenna group of Chalmers Institute of Technology possesses these capabilities through the Bluetest reverberation chamber [24].

This paper is the result of a short-term mission granted by the COST 284. The antenna-design competencies of the LEAT have been combined with the reverberation chamber measurement skills of the antenna group of Chalmers Institute of Technology. Several prototypes have been measured at Chalmers in terms of total efficiency, diversity gain, envelope correlation coefficient, and mean effective gain. Efficiency results are compared with the same measurements obtained through a homemade Wheeler Cap at the LEAT. The envelope correlation coefficient, the MEG, and the MEG ratio calculated from simulated values are also presented and compared [23, 25–27]. We focus on the comparison of the performance of an initial two-antenna system with two different neutralized structures and especially the benefit brought back by the neutralization technique.

2. DESIGNED STRUCTURES AND S-PARAMETER MEASUREMENTS

The multiantenna systems were designed using the electromagnetic software tool IE3D [28]. The initial two-antenna system is presented in Figure 1 (the design procedure was already described in [22]). It consists of two PIFAs symmetrically placed on a $40 \times 100\,\text{mm}^2$ PCB and separated by $0.12\lambda_0$ (18 mm at 2 GHz). They are fed by a metallic strip soldered to an SMA connector and shorted to the PCB by an identical strip. Each PIFA is optimized to cover the UMTS band (1920–2170 MHz) with a return loss goal of −6 dB. The optimized dimensions are of 26.5 mm length and of 8 mm width. A prototype was fabricated using a 0.3-mm-thick nickel silver material (conductivity $\sigma = 4 \times 10^6$ S/m). In Figure 2, we present the simulated and the measured S-parameters of the structure. The absolute value S_{21} reaches a maximum of −5 dB in the middle of the UMTS band.

In the first attempt to improve the isolation between the radiating elements, a suspended line as a neutralization device was inserted between the shorting strips of the two PIFAs (see Figure 3). The optimization of this line was already explained in [21]. Figure 4 shows the S-parameters of this new structure. We can see a good matching and a strong improvement of the isolation in the bandwidth of interest: the measured S_{21} parameter always remains below −15 dB. However, a different isolation can be obtained if we implement the same neutralization technique between the two feeding strips

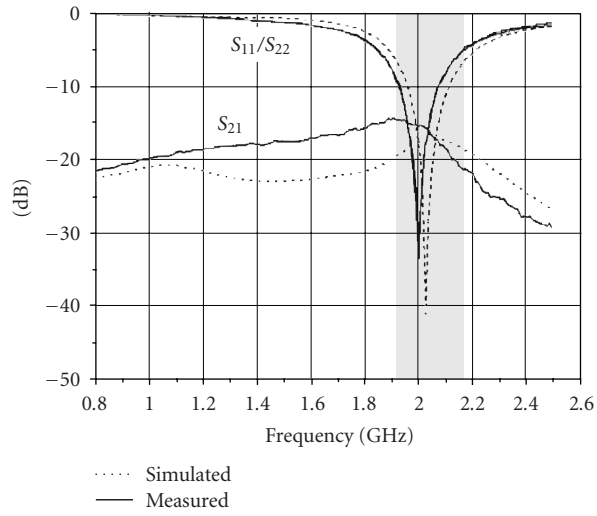

FIGURE 4: Simulated and measured S-parameters of the two-antenna system with a line between the PIFA shorting strips.

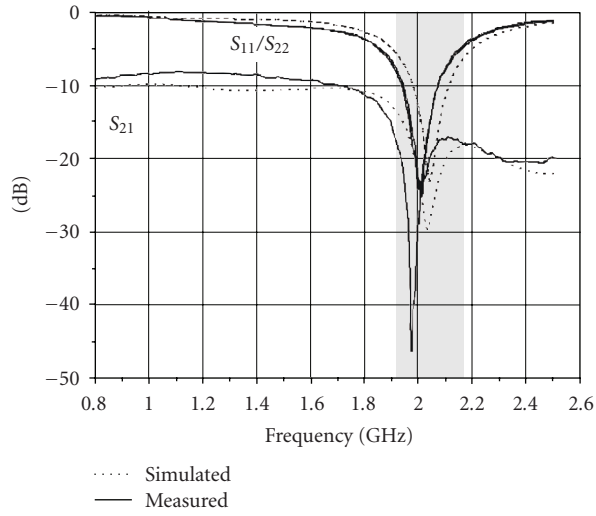

FIGURE 6: Simulated and measured S-parameters of the two-antenna system with the line between the PIFA feeding strips.

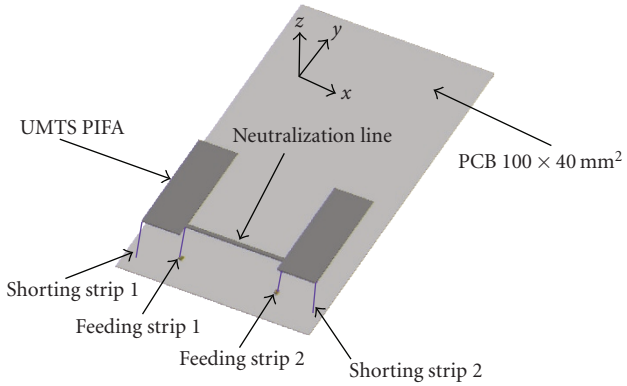

FIGURE 5: 3D view of the two-antenna system with a suspended line between the PIFA feeding strips.

of the PIFAs (see Figure 5). We can observe in Figure 6 that a deep null is now achieved in the middle of the UMTS band. Moreover, the measured S_{21} always remains below −18 dB in the whole UMTS band. All these values seem to be very satisfactory for diversity purposes.

3. COMPARISON OF THE DIVERSITY PERFORMANCE

3.1. *Total efficiency*

Traditionally, the radiation performance of an antenna is measured outdoors or in an anechoic chamber. In order to obtain the total efficiency, we need to measure the radiation pattern in all directions in space and integrate the received power density to find the total radiated power. This gives the total efficiency when compared to the corresponding radiated power of a known reference antenna. This final result is obtained after a long measurement procedure. This parameter can be measured very much faster and easier in a reverberation chamber. However, it is necessary to measure a reference case (a dipole antenna having an efficiency of 96% in our case) and then the antenna system under test (AUT). It is also important that the chamber is loaded in exactly the same way for these both measurements. For the reference case, the transmission between the reference antenna and the excitation antennas is measured in the chamber with the reference antenna in free space that means at least half a wavelength away from any lossy objects and/or the metallic walls of the chamber. As soon as the reference case is completed, we can measure the AUT. From both measurements, we can then compute P_{ref} (1) and P_{AUT} (2):

$$P_{\text{ref}} = \frac{\left|\overline{S_{21,\,\text{ref}}}\right|^2}{\left(1-\left|\overline{S_{11}}\right|^2\right)\left(1-\left|\overline{S_{22,\text{ref}}}\right|^2\right)}, \tag{1}$$

$$P_{\text{AUT}} = \frac{\left|\overline{S_{21,\,\text{AUT}}}\right|^2}{\left(1-\left|\overline{S_{11}}\right|^2\right)\left(1-\left|\overline{S_{22,\,\text{AUT}}}\right|^2\right)}, \tag{2}$$

where $\overline{S_{21}}$ is the averaged transmission power level, $\overline{S_{11}}$ is the free space reflection coefficient of the excitation antenna, and $\overline{S_{22}}$ is the free space reflection coefficient of the reference antenna (or the antenna under test). The $^-$ denotes averaging over n positions of the platform stirrer, polarization stirrer, and mechanical stirrers. The total efficiency can be then calculated from (3)

$$\eta_{\text{tot}} = \left(1-\left|\overline{S_{22,\,\text{AUT}}}\right|^2\right)\frac{P_{\text{AUT}}}{P_{\text{ref}}}. \tag{3}$$

Figure 7 shows the total efficiency in dB of all the antenna systems (without the neutralization line (a), with the line between the feeding strips (b), and with the line between the shorting strips (c)). The simulated curves have been obtained with the help of IE3D which uses the simulated scattering parameters. The experimental curves have been measured in the reverberation chamber and with the help of a homemade Wheeler-Cap setup [16]. With frequency averaging, the standard deviation of the efficiency measurements is

Table 1: Comparison of η_{tot} and the MEG of both antennas of the different structures at $f = 2$ GHz.

	η_{tot} (dB) antenna1		MEG (dB) antenna1		η_{tot} (dB) antenna2		MEG (dB) antenna2	
	Sim.	RC	Sim.	RC	Sim.	RC	Sim.	RC
Initial	−0.816	−0.75	−3.826	−3.75	−0.81	−1.25	−3.826	−4.25
Line between the feeding strips	−0.10	−0.2	−3.11	−3.2	−0.09	−0.5	−3.108	−3.5
Line between the shorting strips	−0.14	−0.35	−3.152	−3.35	−0.14	−0.65	−3.151	−3.65

Table 2: MEG ratio of the antennas for all the prototypes at $f = 2$ GHz.

	MEG1/MEG2
Initial	1,12
Line between the feeding strips	1,07
Line between the shorting strips	1,07

given as +/ − 0.5 dB in the reverberation chamber. The uncertainty of the homemade Wheeler Cap system is assumed to be quite the same. The total efficiency of both antennas from each prototype is presented. It can be seen that they are slightly different in the two measurement cases (dotted lines and solid lines) due to the fact that the fabricated prototypes suffer from small inherent asymmetries. However, only one curve is presented for each simulation case due to perfect symmetries and identical structure on the CAD software. We can observe that all these curves are in a good agreement especially if we compare their maximums. The small frequency shift observed in all the curves with the dotted lines is due to the fact that the antenna was mechanically modified during transportation for measurement, and therefore frequency is detuned. This effect impacts directly the S_{11} and then the frequency location of the maximum of the total efficiency. The improvement brought by the neutralization technique is clearly shown: the maximum total efficiency of the neutralized antennas is around −0.25 dB, whereas the one of the initial structure is less than −1 dB.

3.2. Mean effective gain and mean effective gain ratio

In order to characterize the performance of a multichannel antenna in a mobile environment, different parameters as the MEG and the MEG ratio are used. The total efficiency is the average antenna gain in the whole space. Equation (4) shows that it can be calculated from the integration of the radiation pattern cuts

$$\eta_{\text{tot}} = \frac{\int_0^{2\pi}\int_0^{\pi}\left(G_\theta(\theta,\varphi)+G_\varphi(\theta,\varphi)\right)\sin\theta d\,\theta d\varphi}{4\pi}, \quad (4)$$

where G_θ and G_φ are the antenna power gain patterns.

The MEG is a statistical measure of the antenna gain in a mobile environment. It is equal to the ratio of the mean received power of the antenna and the total mean incident. It can be expressed by (5) as in [6]:

$$\text{MEG} = \int_0^{2\pi}\int_0^{\pi}\left(\frac{\text{XPR}}{1+\text{XPR}}G_\theta(\theta,\varphi)P_\theta(\theta,\varphi) + \frac{1}{1+\text{XPR}}G_\varphi(\theta,\varphi)P_\varphi(\theta,\varphi)\right)\sin\theta d\,\theta d\varphi, \quad (5)$$

where P_θ and P_φ are the angular density functions of the incident power, and XPR represents the cross-polarization power gain which is defined in (6):

$$\text{XPR} = \frac{\int_0^{2\pi}\int_0^{\pi}P_\theta(\theta,\varphi)\sin\theta d\,\theta d\varphi}{\int_0^{2\pi}\int_0^{\pi}P_\varphi(\theta,\varphi)\sin\theta d\,\theta d\varphi}. \quad (6)$$

In the case where the antenna is located in a statistically uniform Rayleigh environment (i.e., the case in the reverberation chamber), we have XPR = 1 and $P_\theta = P_\varphi = 1/4\pi$. The MEG is then equal to the total antenna efficiency divided by two or −3 dB [27]. Moreover, to achieve good diversity gain, the average received power from each antenna element must be nearly equal: this corresponds to getting the ratio of the MEG between the two antennas close to unity [29]. Table 1 presents $\eta_{\text{tot}}$and the MEG of both antennas for the three prototypes at $f = 2$ GHz. The "Sim." values have been computed using the simulated radiation patterns while the reverberation chamber results "RC" are taken from the previous measurements.

The neutralization line provides an enhancement of the η_{tot} and the MEG as expected from the previous values. The improvement of the MEG is about 0.7 dB with regard to the initial structure. Table 2 presents the MEG ratio between the two antennas of the different prototypes (computed from the RC MEG) at 2 GHz. It is seen that the antennas have comparable-average-received power because these entire ratios are close to unity. Such a result was somewhat expected due to the symmetric antenna configuration of our prototypes. In fact, the MEG difference only shows here the prototyping errors we made during the fabrication process. Nevertheless, all the results of this section confirm the benefit of using a neutralization technique between the radiators.

3.3. Correlation

For diversity and MIMO applications, the correlation between the signals received by the antennas at the same side of

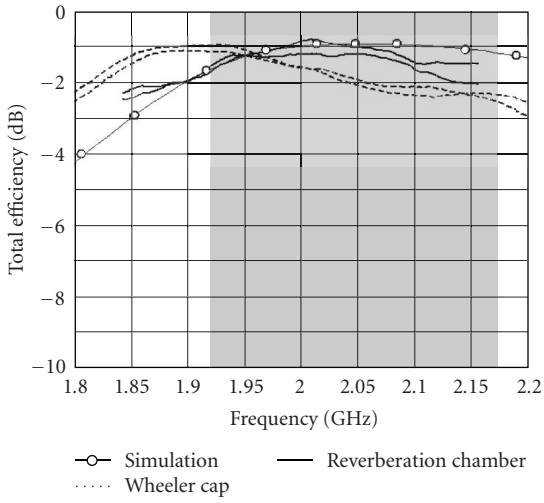

(a)

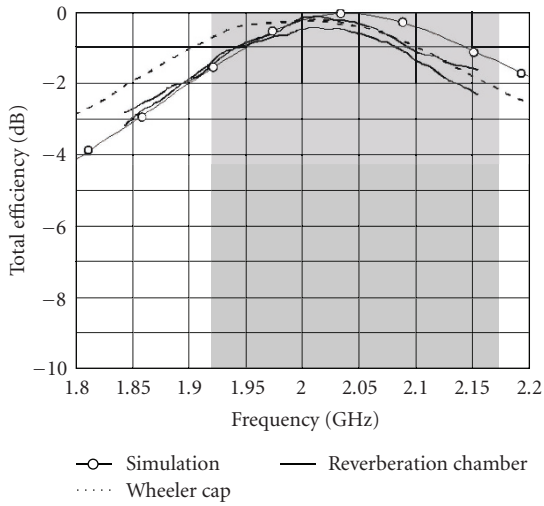

(b)

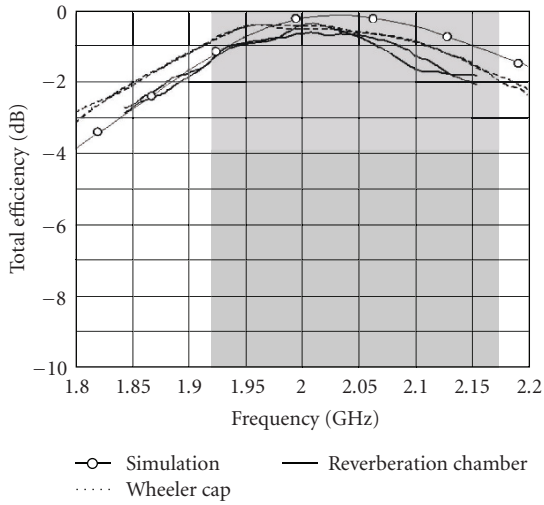

(c)

Figure 7: Total efficiency of the two-antenna structures: (a) without the neutralization line, (b) with the neutralization line between the feeding strips, and (c) with the neutralization line between the shorting strips.

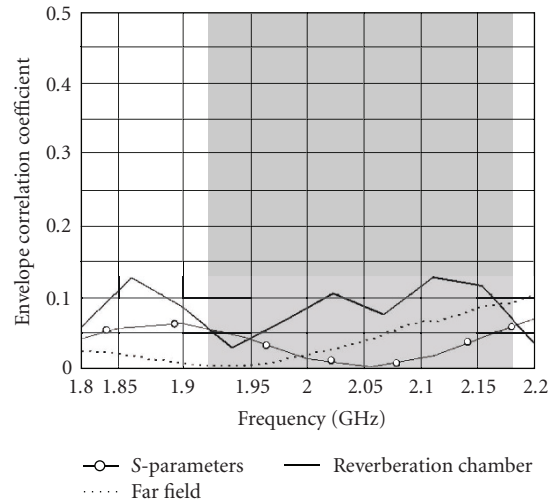

(a)

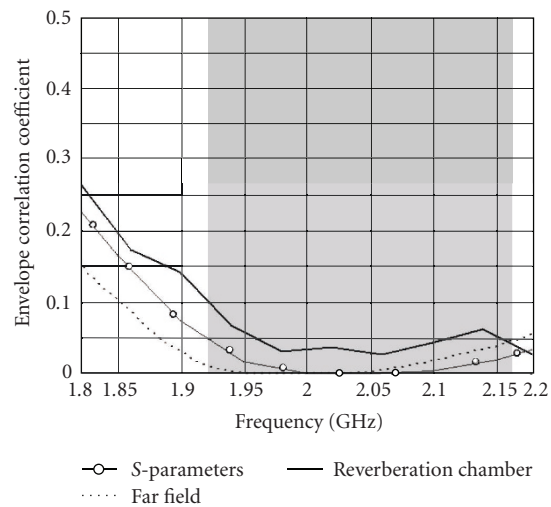

(b)

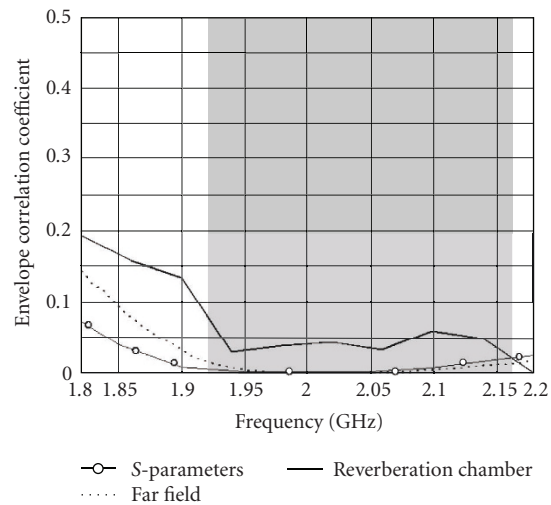

(c)

Figure 8: Envelope correlation coefficient versus frequency of the two-antenna systems: (a) without the neutralization line, (b) with the line between the feeding strips, and (c) with the neutralization line between the shorting strips.

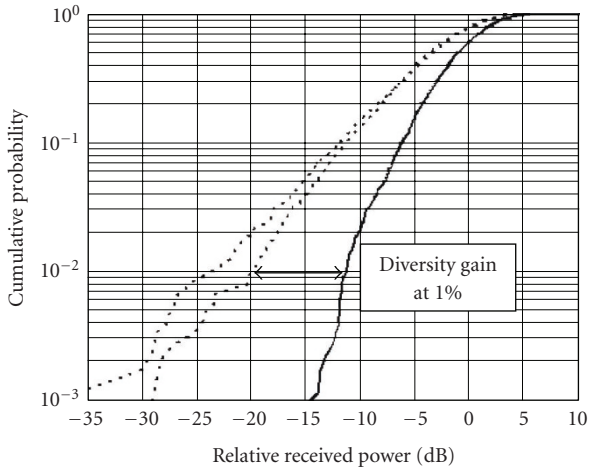

(a)

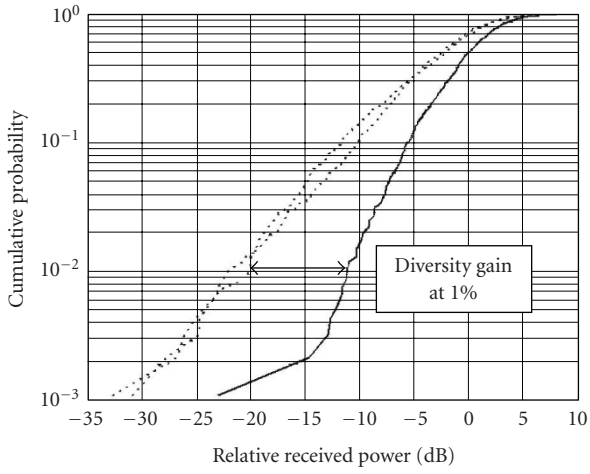

(b)

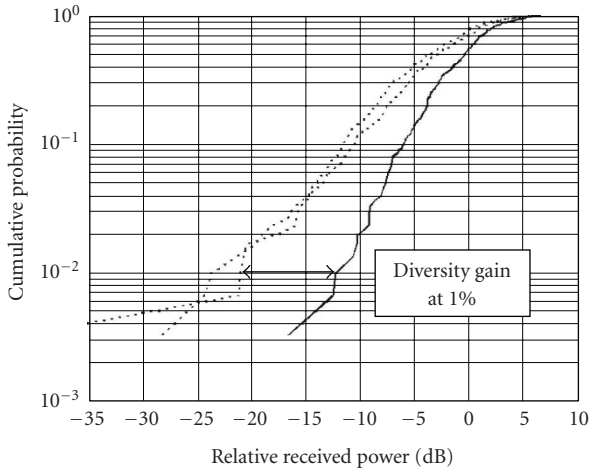

(c)

Figure 9: Cumulative probability of the two-antenna systems over a 4 MHz bandwidth at 2 GHz: (a) without the neutralization line, (b) with the neutralization line between the feeding strips, and (c) with the neutralization line between the shorting strips.

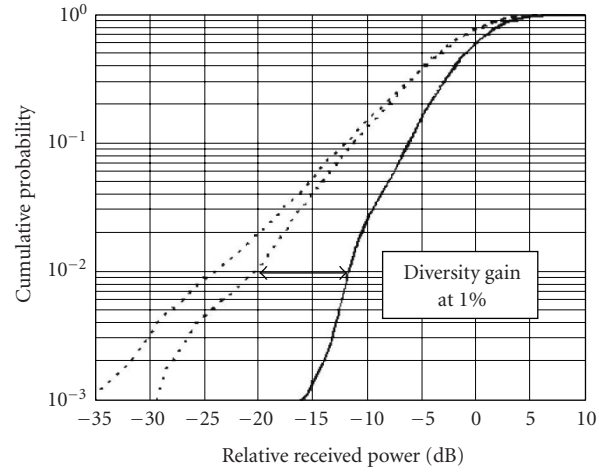

(a)

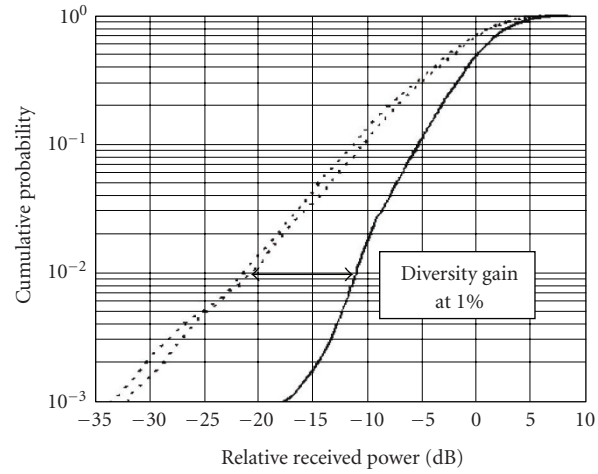

(b)

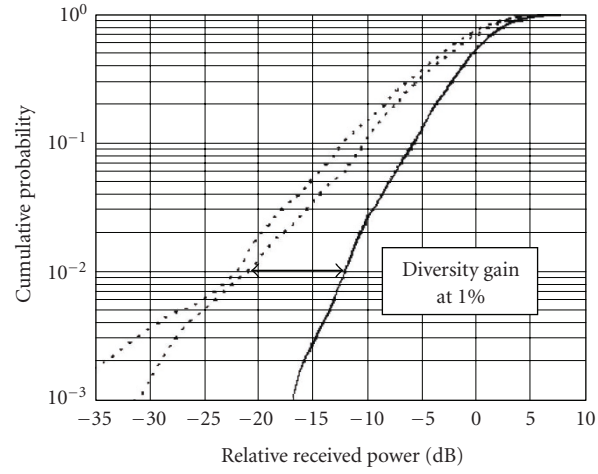

(c)

Figure 10: Smoothed cumulative probability of the two-antenna systems over a 4 MHz bandwidth at 2 GHz: (a) without the neutralization line, (b) with the neutralization line between the feeding strips, and (c) with the neutralization line between the shorting strips.

a wireless link is an important figure of merit. Usually, the envelope correlation is presented to evaluate the diversity capabilities of a multiantenna system [30]. This parameter should be preferably computed from 3D-radiation patterns [31, 32], but the process is tedious because sufficient pattern cuts must be taken into account. In the case of a two-antenna system, the envelope correlation ρ_e is given by (7) as in [31, 32]:

$$\rho_e = \frac{\left| \iint_{4\pi} [\vec{F}_1(\theta,\varphi) \bullet \vec{F}_2^*(\theta,\varphi) d\Omega] \right|^2}{\iint_{4\pi} \left| \vec{F}_1(\theta,\varphi) \right|^2 d\Omega \iint_{4\pi} \left| \vec{F}_2(\theta,\varphi) \right|^2 d\Omega}, \tag{7}$$

where $\vec{F}_i = (\theta, \varphi)$ is the field radiation pattern of the antenna system when the port i is excited, and $\bullet$ denotes the Hermitian product.

However, assuming that the structure will operate in a uniform multipath environment, a convenient and quick alternative consists by using (8) (see [31–33]):

$$\rho_{12} = \frac{\left| S_{11}^* S_{12} + S_{12}^* S_{22} \right|^2}{\left(1 - \left|S_{11}\right|^2 - \left|S_{21}\right|^2\right)\left(1 - \left|S_{22}\right|^2 - \left|S_{12}\right|^2\right)}. \tag{8}$$

It offers a simple procedure compared to the radiation pattern approach, but it should be emphasized that this equation is strictly valid when the three following assumptions are fulfilled:

(i) lossless antenna case that means having antennas with high efficiency and no mutual losses [29, 30];

(ii) antenna system is positioned in a uniform multipath environment which is not strictly the case in real environments, however, the evaluation of some prototypes in different real environments has already shown that there are no major differences in these cases [34];

(iii) load termination of the nonmeasured antenna is 50 Ω. In reality, the radio front-end module does not always achieve this situation, but the 50 Ω evaluation procedure is commonly accepted [35, 36].

All these limitations are clearly showing that in real systems the envelope correlation calculated based on of the help of the S_{ij} parameters is not the exact value, but nevertheless is a good approximation. In addition, it should be noted that antennas with an envelope correlation coefficient less than 0.5 are recognized to provide significant diversity performance [30].

To measure the correlation between the antennas of our systems in the reverberation chamber, each branch is connected to a separate receiver. The two different received signals are recorded, and the envelope correlation can be directly computed. Figure 8 presents the measured envelope correlation coefficients of all the antenna systems. They are compared with those obtained using (7) (computation from the simulated IE3D complex 3D-radiation patterns) and with those obtained using (8) (measured S-parameter values). All these curves are in a moderate agreement, but it can be seen that the envelope correlation coefficients of all the prototypes are always lower than 0.15 on the whole UMTS band: good performance in terms of diversity is thus expected [1]. Here, it is however somewhat difficult to claim that the neutralization technique provides an improvement of the correlation. It seems rather obvious that with such spaced antennas operating in a uniform multipath environment, low correlation is not very difficult to achieve.

3.4. Apparent diversity gain and actual diversity gain

The concept of diversity means that we make use of two or more antennas to receive a signal and that we are able to combine the replicas of the received signal in a desirable way to improve the communication link performance. One requirement is high isolation between the antennas; otherwise the diversity gain will be low. The apparent diversity gain $G_{\text{div app}}$ relative to antenna1 and the actual diversity gain $G_{\text{div act}}$ are defined in (9)

$$\begin{aligned} G_{\text{div app}} &= \frac{S/N}{S_1/N_1}, \\ G_{\text{div act}} &= \frac{S/N}{S_1/N_1}\eta_{\text{tot1}}, \end{aligned} \tag{9}$$

where η_{tot1} is the total efficiency of antenna1.

Note that these formulas are valid only if the noise signals N_1 (and N_2 for the second antenna) are independent of the total efficiency. This is the case if the system noise is dominated by those of the receivers or if the antenna noise temperature is the same as the surrounding temperature. The last condition is often close to being satisfied in mobile systems because the antenna is rather omnidirectional and picks up thermal noise mainly from the environment (ground, buildings, trees, human) around the antenna, and less from the low sky temperature.

We can see in Figure 9 the power samples of each two-antenna system (without the neutralization line (a), with the line between the feeding strips (b), and with the line between the shorting strips (c)) averaged over a 20-MHz frequency band at 2 GHz. We can observe that the combined signal curves with the selection combining scheme (solid lines) are steeper than the two curves of the antenna elements taken alone (dotted lines). This is the benefit of combining the two signals received by each antenna of the structure. By just looking at the curves in Figure 9, the uncertainty is undoubtedly very large. This is due to the obvious lack of samples at low-probability levels coming from the measurement procedure.

The apparent diversity gain is determined by the power-level improvement at a certain probability level. In Figures 9(a), 9(b), and 9(c), we have chosen 1% probability. It is then the difference between the strongest antenna element curve and the combined signal curve. The power improvement is 7.6 dB for the system with low isolation, whereas it is 8.8 dB and 9.1 dB for the system with high isolation, respectively, for the line between the shorting strips and the line between the feeding strips. As the total efficiency is not taken into account in the apparent diversity gain, the improvement only comes from the fact that the radiation patterns are slightly different in the case of the two neutralized structures. Especially, an increase of the cross-polarization level occurs in the radiation patterns of the neutralized structures due to the

Table 3: Summary of the measured and computed diversity gains of all the antenna systems.

Prototypes	Total efficiency best branch	Apparent diversity gain	Apparent diversity gain, smooth curved	Actual diversity gain	Actual diversity gain, smooth curved
Without any line	−0.75 dB	7.6 dB	8.6 dB	6.3 dB	7.8 dB
Shorting strips link	−0.35 dB	8.8 dB	9.2 dB	8 dB	8.8 dB
Feeding strips link	−0.2 dB	9.1 dB	9.75 dB	8.6 dB	9.5 dB

fact that a strong current is flowing on the line. This increase of the X-pol appears to be beneficial for the diversity gain. When taking into account the total efficiency of the antennas, we can compute the actual diversity gain as 6.3 dB for the initial system, 8 dB and 8.6 dB for the neutralized shorting strips and feeding strips systems, respectively. The data from Figure 9 were also processed with the smooth function of MATLAB [37] in order to evaluate the validity of our measurements. Several "smooth steps" were tried out in this operation and the new curves are presented in Figure 10. It appears that all the apparent diversity gains were formerly underestimated. The new actual diversity gains are now 7.8 dB, 8.8 dB, and 9.5 dB for, respectively, the initial, the neutralized shorting strips and feeding strips systems. A summary of all these values can be found in Table 3.

It seems obvious that the neutralization technique enhances the actual diversity gain. These results are consistent with other publications [38] and even better due to the use of highly efficient antennas here. We should also point out that the apparent diversity gain and the actual diversity gain are not so much different due to the same reason [39].

4. CONCLUSION

In this paper, we have presented different two-antenna systems with poor and high isolations for diversity purposes. The reverberation chamber measurements at the antenna group of Chalmers University of Technology have shown that even if the envelope correlation coefficient of these systems is very low, having antennas with high isolation will improve the total efficiency and the effective diversity gain of the system. The same conclusions have been drawn regarding the MEG values. All these results point out the usefulness of our simple solution to achieve efficient antenna systems at the terminal side of a wireless link for diversity or MIMO applications. Next studies will focus on the effect of the users upon the neutralization technique by positioning the antenna systems next to a phantom head.

ACKNOWLEDGMENT

The authors express their gratitude to the COST284 project for providing the opportunity to make a short-term scientific mission from the LEAT to Chalmers Institute.

REFERENCES

[1] Z. Ying and D. Zhang, "Study of the mutual coupling, correlations and efficiency of two PIFA antennas on a small ground plane," in *Proceedings of IEEE Antennas and Propagation Society International Symposium*, vol. 3, pp. 305–308, Washington, DC, USA, July 2005.

[2] J. Thaysen and K. B. Jakobsen, "MIMO channel capacity versus mutual coupling in multi antenna element system," in *Proceedings of the 26th Annual Meeting & Symposium on Antenna Measurement Techniques Association (AMTA '04)*, Stone Mountain, Ga, USA, October 2004.

[3] M. Karakoikis, C. Soras, G. Tsachtsiris, and V. Makios, "Compact dual-printed inverted-F antenna diversity systems for portable wireless devices," *IEEE Antennas and Wireless Propagation Letters*, vol. 3, no. 1, pp. 9–14, 2004.

[4] K.-L. Wong, C.-H. Chang, B. Chen, and S. Yang, "Three-antenna MIMO system for WLAN operation in a PDA phone," *Microwave and Optical Technology Letters*, vol. 48, no. 7, pp. 1238–1242, 2006.

[5] S. H. Chae, S.-K. Oh, and S.-O. Park, "Analysis of mutual coupling, correlations, and TARC in WiBro MIMO array antenna," *IEEE Antennas and Wireless Propagation Letters*, vol. 6, pp. 122–125, 2007.

[6] H. T. Hui, "Practical dual-helical antenna array for diversity/MIMO receiving antennas on mobile handsets," *IEE Proceedings: Microwaves, Antennas and Propagation*, vol. 152, no. 5, pp. 367–372, 2005.

[7] J. Villanen, P. Suvikunnas, C. Icheln, J. Ollikainen, and P. Vainikainen, "Advances in diversity performance analysis of mobile terminal antennas," in *Proceedings of the International Symposium on Antennas and Propagation (ISAP '04)*, Sendai, Japan, August 2004.

[8] M. Manteghi and Y. Rahmat-Samii, "Novel compact tri-band two-element and four-element MIMO antenna designs," in *Proceedings of the International Symposium on Antennas and Propagations (ISAP '06)*, pp. 4443–4446, Albuquerque, NM, USA, July 2006.

[9] M. Manteghi and Y. Rahmat-Samii, "A novel miniaturized triband PIFA for MIMO applications," *Microwave and Optical Technology Letters*, vol. 49, no. 3, pp. 724–731, 2007.

[10] D. Browne, M. Manteghi, M. P. Fits, and Y. Rahmat-Samii, "Experiments with compact antenna arrays for MIMO radio communications," *IEEE Transaction on Antennas and Propagation*, vol. 54, no. 11, part 1, pp. 3239–3250, 2007.

[11] B. Lindmark and L. Garcia-Garcia, "Compact antenna array for MIMO applications at 1800 and 2450 MHz," *Microwave and Optical Technology Letters*, vol. 48, no. 10, pp. 2034–2037, 2006.

[12] R. G. Vaughan and J. B. Andersen, "Antenna diversity in mobile communications," *IEEE Transactions on Vehicular Technology*, vol. 36, no. 4, pp. 149–172, 1987.

[13] B. K. Lau, J. B. Andersen, G. Kristensson, and A. F. Molisch, "Impact of matching network on bandwidth of compact antenna arrays," *IEEE Transactions on Antennas and Propagation*, vol. 54, no. 11, pp. 3225–3238, 2006.

[14] J. B. Andersen and B. K. Lau, "On closely coupled dipoles in a random field," *IEEE Antennas and Wireless Propagation Letter*, vol. 5, no. 1, pp. 73–75, 2006.

[15] J. W. Wallace and M. A. Jensen, "Termination-dependent diversity performance of coupled antennas: network theory analysis," *IEEE Transactions on Antennas and Propagation*, vol. 52, no. 1, pp. 98–105, 2004.

[16] M. A. J. Jensen and J. W. Wallace, "A review of antennas and propagation for MIMO wireless communications," *IEEE Transactions on Antennas and Propagation*, vol. 52, no. 11, pp. 2810–2824, 2004.

[17] J. Thaysen and K. B. Jakobsen, "Mutual coupling reduction using a lumped LC circuit," in *Proceedings of the 13th International Symposium on Antennas (JINA '04)*, pp. 492–494, Nice, France, November 2004.

[18] S. Dossche, S. Blanch, and J. Romeu, "Optimum antenna matching to minimise signal correlation on a two-port antenna diversity system," *IET Electronics Letters*, vol. 40, no. 19, pp. 1164–1165, 2004.

[19] S. Dossche, J. Rodriguez, L. Jofre, S. Blanch, and J. Romeu, "Decoupling of a two-element switched dual band patch antenna for optimum MIMO capacity," in *Proceedings of the International Symposium on Antennas and Propagations (ISAP '06)*, pp. 325–328, Albuquerque, NM, USA, July 2006.

[20] Y. Gao, X. Chen, C. Parini, and Z. Ying, "Study of a dual-element PIFA array for MIMO terminals," in *Proceedings of the International Symposium on Antennas and Propagations (ISAP '06)*, pp. 309–312, Albuquerque, NM, USA, July 2006.

[21] A. Diallo, C. Luxey, P. Le Thuc, R. Staraj, and G. Kossiavas, "Study and reduction of the mutual coupling between two mobile phone PIFAs operating in the DCS1800 and UMTS bands," *IEEE Transactions on Antennas and Propagation*, vol. 54, no. 11, part 1, pp. 3063–3074, 2006.

[22] A. Diallo, C. Luxey, P. Le Thuc, R. Staraj, and G. Kossiavas, "Enhanced diversity antennas for UMTS handsets," in *Proceedings of the European Conference on Antennas and Propagations (EuCAP '06)*, Nice, France, November 2006.

[23] P.-S. Kildal and K. Rosengren, "Correlation and capacity of MIMO systems and mutual coupling, radiation efficiency, and diversity gain of their antennas: simulations and measurements in a reverberation chamber," *IEEE Communications Magazine*, vol. 42, no. 12, pp. 104–112, 2004.

[24] http://www.bluetest.se/.

[25] T. Bolin, A. Derneryd, G. Kristensson, V. Plicanic, and Z. Ying, "Two-antenna receive diversity performance in indoor environment," *Electronics Letters*, vol. 41, no. 22, pp. 1205–1206, 2005.

[26] T. Taga, "Analysis for mean effective gain of mobile antennas in land mobile radio environments," *IEEE Transactions on Vehicular Technology*, vol. 39, no. 2, pp. 117–131, 1990.

[27] K. Kalliola, K. Sulonen, H. Laitinen, O. Kivekäs, J. Krogerus, and P. Vainikainen, "Angular power distribution and mean effective gain of mobile antenna in different propagation environments," *IEEE Transactions on Vehicular Technology*, vol. 51, no. 5, pp. 823–838, 2002.

[28] IE3D, Release 11.15, Zeland software, 2005.

[29] C. C. Chlau, X. Chen, and C. Q. Parinl, "A compact four-element diversity-antenna array for PDA terminals in a mimo system," *Microwave and Optical Technology Letters*, vol. 44, no. 5, pp. 408–412, 2005.

[30] S. C. K. Ko and R. D. Murch, "Compact integrated diversity antenna for wireless communications," *IEEE Transactions on Antennas and Propagation*, vol. 49, no. 6, pp. 954–960, 2001.

[31] I. Salonen and P. Vainikainen, "Estimation of signal correlation in antenna arrays," in *Proceedings of the 12th International Symposium Antennas (JINA '02)*, vol. 2, pp. 383–386, Nice, France, November 2002.

[32] P. Brachat and C. Sabatier, "Réseau d'antennes à 6 Capteurs en Diversité de Polarisation," in *Proceedings of the 13th International Symposium Antennas (JINA '04)*, Nice, France, November 2004.

[33] J. Thaysen and K. B. Jakobsen, "Envelope correlation in (N, N) MIMO antenna array from scattering parameters," *Microwave and Optical Technology Letters*, vol. 48, no. 5, pp. 832–834, 2006.

[34] Z. Ying, V. Plicanic, T. Bolin, G. Kristensson, and A. Derneryd, "Characterization of Multi-Channel Antenna Performance for Mobile Terminal by Using Near Field and Far Field Parameters," COST 273 TD (04)(095), Göteborg, Sweden, June 2004.

[35] A. Derneryd and G. Kristensson, "Signal correlation including antenna coupling," *Electronics Letters*, vol. 40, no. 3, pp. 157–159, 2004.

[36] A. Derneryd and G. Kristensson, "Antenna signal correlation and its relation to the impedance matrix," *Electronics Letters*, vol. 40, no. 7, pp. 401–402, 2004.

[37] http://www.mathworks.fr/.

[38] K. Rosengren and P.-S. Kildal, "Diversity performance of a small terminal antenna for UMTS," in *Proceedings of Nordic Antenna Symposium (Antenn '03)*, Kalmar, Sweden, May 2003.

[39] P.-S. Kildal, K. Rosengren, J. Byun, and J. Lee, "Definition of effective diversity gain and how to measure it in a reverberation chamber," *Microwave and Optical Technology Letters*, vol. 34, no. 1, pp. 56–59, 2002.